

1 **Measurement Report: A Multi-Year Study on the Impacts of Chinese New Year Celebrations on Air**
2 **Quality in Beijing, China.**

3
4 Benjamin Foreback^{1,2}, Lubna Dada², Kaspar R. Daellenbach², Chao Yan^{1,2}, Lili Wang³, Biwu Chu^{2,4}, Ying
5 Zhou¹, Tom V. Kokkonen^{2,6}, Mona Kurppa⁷, Rosaria E. Pileci⁵, Yonghong Wang², Tommy Chan², Juha
6 Kangasluoma^{1,2}, Lin Zhuohui¹, Yishou Guo¹, Chang Li¹, Rima Baalbaki², Joni Kujansuu^{1,2}, Xiaolong Fan¹,
7 Zemin Feng¹, Pekka Rantala², Shahzad Gani², Federico Bianchi^{1,2}, Veli-Matti Kerminen², Tuukka Petäjä^{1,2,6},
8 Markku Kulmala^{1,2,6}, Yongchun Liu¹ and Pauli Paasonen²

9
10 ¹Aerosol and Haze Laboratory, Beijing Advanced Innovation Center for Soft Matter Science and Engineering,
11 Beijing University of Chemical Technology, Beijing, China

12 ²Institute for Atmospheric and Earth System Research / Physics, Faculty of Science, University of Helsinki,
13 Finland

14 ³Institute of Atmospheric Physics, Chinese Academy of Sciences, Beijing, China

15 ⁴State Key Joint Laboratory of Environment Simulation and Pollution Control, Research Center for Eco-
16 Environmental Sciences, Chinese Academy of Sciences, Beijing 100085, China

17 ⁵U-Earth Biotech Ltd., London, United Kingdom

18 ⁶Joint International Research Laboratory of Atmospheric and Earth System Sciences, School of Atmospheric
19 Sciences, Nanjing University, Nanjing, China

20 ⁷Atmospheric Composition Research, Finnish Meteorological Institute, Helsinki, Finland

21
22 Corresponding Author: Pauli Paasonen

23
24 Correspondence to: Pauli Paasonen (pauli.paasonen@helsinki.fi)

25
26 **ABSTRACT**

27 This study investigates the influence of the Chinese New Year (CNY) celebrations on local air quality in Beijing
28 from 2013 through 2019. CNY celebrations include burning of fireworks and firecrackers, which consequently
29 has a significant short-term impact on local air quality. In this study, we bring together comprehensive
30 observations at the newly-constructed Aerosol and Haze Laboratory at Beijing University of Chemical
31 Technology – West Campus (BUCT-AHL) and hourly measurements from twelve Chinese government air
32 quality measurement stations throughout the Beijing metropolitan area. These datasets are used together to
33 provide a detailed analysis of air quality during the CNY over multiple years, during which the city of Beijing
34 prohibited the use of fireworks and firecrackers in an effort to reduce air pollution before CNY 2018. Datasets
35 used in this study include particulate matter mass concentrations (PM_{2.5} and PM₁₀), trace gases (NO_x, SO₂, O₃,
36 and CO) and meteorological variables for 2013-2019, aerosol particle size distributions, and concentrations of
37 sulfuric acid and black carbon for 2018 and 2019. Studying the CNY over several years, which has rarely been
38 done in previous studies, can show trends and effects of societal and policy changes over time, and the results
39 can be applied to study problems and potential solutions of air pollution resulting from holiday celebrations.
40 Our results show that during the 2018 CNY, air pollutant concentrations peaked during the CNY night (for
41 example, PM_{2.5} reached a peak around midnight of over 250 µg/cm³, compared to values of less than 50 µg/cm³
42 earlier in the day). The pollutants with the most notable spikes were sulfur dioxide, particulate matter, and
43 black carbon, which are emitted in burning of firework and firecrackers. Sulfuric acid concentration followed
44 the sulfur dioxide concentration and showed elevated overnight concentration. Analysis of aerosol particle
45 number size distribution showed direct emissions of particles with diameters around 100 nm in relation to
46 firework burning. During the 2019 CNY, the pollution levels were somewhat lower (PM_{2.5} peaking to around
47 150 µg/cm³ at CNY compared to values around 100 µg/cm³ earlier in the day) and only minor peaks related to

48 firework burning were observed. During both CNYs 2018 and 2019 secondary aerosol formation in terms of
49 particle growth was observed. Meteorological conditions were comparable between these two years, suggesting
50 that CNY-related emissions were less in 2019 compared to 2018. During the 7-year study period, it appears
51 that there has been a general decrease in CNY-related emissions since 2016. For example, peak in $PM_{2.5}$ in
52 2016 was over $600 \mu\text{g}/\text{cm}^3$, and in the years following, the peak was less each year, with a peak around 150
53 $\mu\text{g}/\text{cm}^3$ in 2019. This is indicative of the restrictions and public awareness of the air quality issues having a
54 positive effect on improving air quality during the CNY. Going into the future, long-term observations will
55 offer confirmation for these trends.

56

57 **1 INTRODUCTION**

58

59 Anthropogenic emissions associated with festivities, notably fireworks and firecrackers (hereafter simply
60 fireworks), are known for their hazardous effects, and even short-term exposure can have significant impacts
61 on human health (Bach et al., 2007; Chen et al., 2011; Jiang et al., 2015; Yang et al., 2014). Firework
62 celebrations are found to increase the concentrations of trace gases and particle concentrations (Kong et al.,
63 2015; Li et al., 2013). Furthermore, some studies have related these festivities to the occurrence of haze
64 episodes in the days following a firework event (Li et al., 2013; Feng et al., 2012).

65

66 The Chinese New Year (CNY) is a traditional annual holiday occurring in wintertime – in January or in
67 February as the exact date is based on the lunar cycle. Because of the adverse impacts on health, pollution from
68 fireworks during the CNY has gathered attention worldwide. For instance, studies including Yang et al. (2014)
69 in Jinan, Shi et al. (2014) in Tianjin, and Feng et al. (2012) and Zhang et al. (2010) in Shanghai have shown
70 that there is noticeable degradation in air quality associated with Chinese New Year celebrations in these cities.
71 Wang et al. (2007) has shown that firework celebrations emit significant amounts of sulfur dioxide and black
72 carbon. The effects of fireworks on air pollution are known for various holidays in other countries as well.
73 Studies in India, for example, during the country’s annual Diwali Festival in the late autumn have also shown
74 results of high pollution from firework use (Ravindra et al., 2003; Mönkkönen et al., 2004; Barman et al., 2007;
75 Singh et al., 2009; Yerramesetti et al., 2013). As another example, a study by Liu et al. (1997) in Southern
76 California, USA showed enhanced concentrations of particulate matter and trace gas pollutants during firework
77 celebrations.

78

79 Because of the rising awareness of air quality problems during holiday celebrations, the government of Beijing
80 decided to implement a prohibition on firework burning within the 5th Ring Road of Beijing, in an effort to
81 reduce air pollution, described in a study by Liu et al. (2019). Their study reported that the prohibition resulted
82 in about a 40% decrease in the total number of fireworks and firecrackers sold in the city of Beijing during the
83 2018 CNY holiday compared to 2016. Furthermore, Liu et al. (2019) reported that observed concentrations of
84 air pollutants during the 2018 CNY was significantly less than that in 2016.

85

86 Therefore, an aim of this study is to confirm the conclusions of the Liu et al. (2019) study, using not only a
87 2016 vs. 2018 comparison, but a longer study of each year between 2013 and 2019. Furthermore, this study
88 offers a spatial comparison of the area where fireworks were prohibited (inside the 5th ring) with a region where
89 there was no prohibition (outside the ring). Currently, there are no previous studies that perform such a side-
90 by-side comparison of areas with different firework burning policies.

91

92 This manuscript provides a detailed view on how CNY celebrations have influenced air quality and atmospheric
93 chemistry in the Beijing metropolitan area. We start with an in-depth analysis of data from 2018 and 2019, and
94 then we expand with the longer 7-year dataset. Combined, these datasets provide perspective into the impacts
95 of the imposed restrictions on firework use in the Beijing area. The specific questions we aim to answer include:
96 1.) how the CNY celebrations and associated increase in precursor and aerosol emissions reflect in the

97 atmospheric concentrations of trace gases and particulate matter and particle number size distribution; 2.) how
98 these changes are connected with meteorological conditions; 3.) how the influence of CNY affects regional air
99 quality variation spatially over the Beijing area; and 4.) how the influence of CNY on Beijing air quality has
100 changed during the recent years, including the result of the firework prohibition beginning in 2018.

101

102 **2 METHODS**

103

104 The observations used in this study include measurements collected from the Beijing University of Chemical
105 Technology, Aerosol and Haze Laboratory (BUCT-AHL), an academic research station in Beijing China (Liu
106 et al., 2020); along with seven years of data from twelve measurement stations throughout the Beijing
107 metropolitan area, operated by the Chinese Ministry of Environmental Protection (MEP). The long-term
108 datasets also provide spatial context in the scale of the greater Beijing area, including a comparison of
109 measurements inside versus outside of the prohibition area. Here we investigated years 2013-2019. Although
110 data from the 2020 CNY is available, we have decided not to include it in this study because of the widespread
111 impacts of the COVID-19 virus that affected China during this time. Due to the unfortunate circumstance, many
112 Chinese citizens refrained from travel, public celebrations and time spent in public. Consequently, the 2020
113 CNY is not directly comparable to previous years.

114

115 This study is novel and unique in a few ways. First, it is one of only a few studies to not only show
116 measurements for a single CNY (or similar celebratory holidays in other countries), but it studies the holiday
117 over seven continuous years. This offers the ability to show trends and effects of, for example policy changes,
118 over time. Furthermore, this study uses data from multiple institutions, which demonstrates the value of
119 collaborations between different institutions when it comes to solving major global problems such as air
120 pollution. This study also compares the CNY inside the centre of the city to the greater Beijing area, which is
121 unique compared to any previous CNY (or similar holiday) air quality study that uses data at a single location.
122 Our insights offer value to scientists and policy makers around the world who are interested in improving air
123 quality during holidays that involve firework celebrations. Improving air quality, even short-term, can have a
124 significant positive impact on health and wellbeing of citizens.

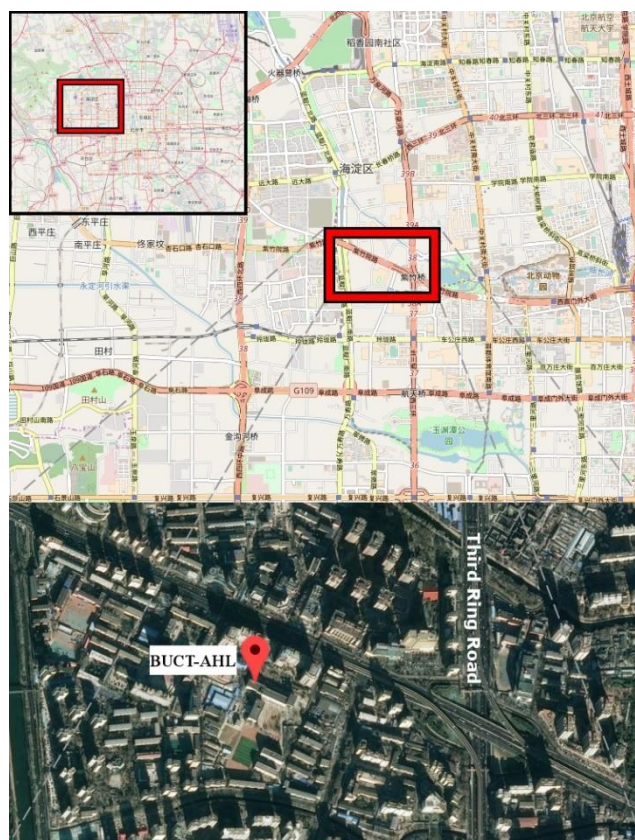
125

126 **2.1 Measurement sites**

127

128 This study uses data collected from two sources. First, we used data from the newly constructed station near
129 the third ring road of Beijing (39°56'N, 116°17'E; Figure 1; Liu et al., 2020). The station, known as the Aerosol
130 and Haze Laboratory, is located at Beijing University of Chemical Technology West Campus, on the roof of a
131 five-floor building nearby to a busy highway. The station (BUCT-AHL) follows the concept of the Station for
132 Measuring Ecosystem-Atmosphere Relations (SMEAR) in Hyytiälä, Southern Finland (Hari and Kulmala,
133 2005). BUCT-AHL was built in collaboration with the Institute of Atmospheric and Earth System Research
134 (INAR) at the University of Helsinki as part of the effort to build a global SMEAR network (Kulmala, 2018),
135 with the aim to understand atmospheric chemical cocktail in megacity (Kulmala, 2015). In addition to collecting
136 data for in-depth air quality analysis, this joint work increases collaboration between atmospheric scientists in
137 China and Finland.

138



139
 140
 141 **Figure 1:** Location of the BUCT-AHL site within the Beijing metropolitan area. © OpenStreetMap
 142 contributors YEAR. Distributed under the Open Data Commons Open Database License (ODbL)
 143 v1.0.

144
 145 In our analysis, the following datasets from BUCT-AHL during the 2018 and 2019 CNY are used: 1) Trace gas
 146 concentrations: nitrogen oxides (NO_x), sulfur dioxide (SO_2), ozone (O_3), and carbon monoxide (CO); 2) Black
 147 carbon mass concentration (BC); 3) Sub-micron aerosol particle number size distributions; 4) Gas-phase
 148 sulfuric acid (H_2SO_4) concentration; 5) Meteorological observations. Technical details of the instruments,
 149 including manufacturer, parameters measured, time resolution, and available time periods of measurements,
 150 can be found in Table S2 in Supplementary material. These details are also described in Liu et al. (2020).
 151

152 Additionally, we obtained datasets from several national air quality monitoring sites within the Beijing
153 metropolitan area (NAQMS; Song et al., 2017; Tao et al., 2016). These datasets were obtained from the Chinese
154 Ministry of Environmental Protection (MEP), which contain the following: 1) Fine and coarse particulate
155 matter mass concentrations (PM_{2.5} and PM₁₀), 2) trace gases (NO_x, SO₂, O₃, and CO) from 2013 through 2019
156 for a multi-year comparison. This also provided insights into the spatial variability within the Beijing city and
157 particularly contrasting the area where the ban for the fireworks was implemented against the urban background
158 air quality.

159

160 **2.2 Instrumentation**

161

162 **2.2.1 Observations in BUCT-AHL station**

163

164 **Trace gas measurements**

165 Concentrations of carbon monoxide (CO), sulfur dioxide (SO₂), ozone (O₃) and nitrogen oxides (NO_x) were
166 measured with Thermo Environmental Instruments models 48i, 43i-TLE, 42i, and 49i, respectively. They were
167 sampled through a common inlet through the roof of the building. The length of the sampling tube was
168 approximately 3 m long (Zhou et al., 2020). The time resolution of the measurements was 5 minutes, but to be
169 consistent with the MEP datasets, one-hour averages were used in this study.

170

171 **Meteorological observations**

172 Meteorological datasets for 2018-2019 at BUCT-AHL were collected with a Vaisala automatic weather station,
173 AWS310, including wind speed and direction, ambient air temperature and relative humidity. Boundary layer
174 height (BLH) was measured using a Vaisala CL-51 ceilometer. Meteorological and BLH measurements were
175 taken on the rooftop of BUCT-AHL.

176

177 Archived meteorological data for Beijing from 2013-2017 was obtained from the Weather Underground
178 website (<https://www.wunderground.com/history/daily/cn/beijing/ZBNY/>). The station used is the Beijing
179 Nanyuan Airport (ICAO identifier ZBNY), a small airport located between the 4th and 5th Ring Road, south of
180 Beijing city center. The station is approximately 17 km from BUCT-AHL.

181

182 **Sub-micron aerosol particle number size distributions and total number concentrations**

183 Particle size distribution (PSD) between 3 nm and 1 μm was measured using an instrument of the same name,
184 PSD (Liu et al., 2016). The instrument is composed of a nano-scanning mobility particle sizer (nano-SMPS, 3–
185 55 nm, mobility diameter), a long SMPS (25–650 nm, mobility diameter) and an aerodynamic particle sizer
186 (APS, 0.55–10 μm, aerodynamic diameter). It was fitted with a cyclone to remove particles larger than 10 μm
187 from entering the system. Sampling was done from the rooftop using a 3 m long sampling tube. Additional
188 information about the setup of these instruments can be found in Zhou et al. (2020).

189

190 Aerosol particle sizes have been further divided into four modes, based on particle diameter: cluster mode (sub-
191 3 nm), nucleation mode (3–25 nm), Aitken mode (25–100 nm), and accumulation mode (100–1000 nm). The
192 method is described in Zhou et al. (2020).

193

194 **Gas-phase sulfuric acid**

195 Sulfuric acid was measured by a chemical ionization atmospheric-pressure interface time-of-flight mass
196 spectrometer equipped with a nitrate chemical ionization source (CI-APi-TOF, Jokinen et al., 2012). The
197 ionization was done with NO₃⁻ as the reagent ion in ambient pressure (e.g., Petäjä et al., 2009). Nitrate reagent
198 ions were produced by ionizing a mixture of 3 mL.min⁻¹ ultrahigh purity nitrogen flow containing nitric acid
199 with 20 mL.min⁻¹ zero air with an X-ray source. This mixture acted as the sheath flow and was introduced into

200 a coaxial laminar flow reactor concentric to the sample flow. The sample flow was 8.8 L min⁻¹ but only 0.8
201 L.min⁻¹ was drawn into the pinhole of the TOF. The sampling line was 1.6 m long stainless-steel tube having
202 an inner diameter of 3/4 inch and positioned horizontally. The instrument was calibrated with known
203 concentrations of sulfuric acid. Further information about the calibration procedure can be found in Kürten et
204 al. (2012).

205

206 **Black carbon mass concentration**

207 An aethalometer AE33 (Magee Scientific) monitored the light absorption related to the aerosol. Equivalent
208 black carbon (eBC) was computed based on the change in time of the light attenuation using procedures
209 presented in Virkkula et al. (2015).

210

211

212 **2.2.2 Chinese MEP Data**

213

214 Beginning in 2013, the Chinese Ministry of Environmental Protection (MEP) began installing a China-wide
215 network of air quality monitoring stations to measure local and regional air quality. Real-time datasets from
216 this sensor network are published hourly by the China Environmental Monitoring Center (CEMC), which
217 includes PM₁₀, PM_{2.5}, SO₂, NO_x and CO. There are over 1000 active sensors across China (Song et al., 2017;
218 Tao et al., 2016).

219

220 In this study, data from 12 MEP sites throughout Beijing are used (See Table 1 in Supplementary Information
221 for a list of these sites and their locations). The Guanyuan (GY) site is the closest site to BUCT-AHL, about 5
222 km east. The original data are available at <http://106.37.208.233:20035/> and for this study we have removed
223 the outliers with criteria presented by Wu et al. (2018).

224 **2.2.3 Back-trajectories with Hysplit**

225

226 Back trajectories to the BUCT-station were calculated using Hybrid Single-Particle Lagrangian Integrated
227 Trajectory (Hysplit). This model is developed by National Oceanic and Atmospheric Administration (NOAA)
228 Air Resources Laboratory and the Australian Bureau of Meteorology Research Centre, and it is one of the most
229 widely-used models to determine the origin of an air mass (Stein et al., 2015). In this work, Hysplit trajectories
230 were calculated for the CNY each year from 2013-2019, with the trajectories arriving between 18:00 and 06:00
231 local time (UTC+8) during the CNY. This adds value to the analysis in two ways: First, it can show whether
232 the air masses in Beijing originated over other urban areas in China, e.g. the greater Beijing-Tianjin-Hebei
233 (BTH) area, or whether the air mass came from more rural areas, e.g. Inner Mongolia or Mongolia.
234 Additionally, it gives a synoptic overview of the weather conditions leading up to CNY. This in turn provides
235 information on whether the air mass is more stagnant within the BTH area, which would result in higher
236 pollution buildup, or whether it originated farther away, which would mean it would be cleaner from the start
237 (Wang et al., 2010; Chen et al., 2015; Zhu et al., 2020).

238

239 **3 RESULTS AND DISCUSSION**

240

241 Higher atmospheric concentrations due to elevated pollutant emissions during the Chinese New Year were
242 observed both at BUCT-AHL and the MEP sites during the analysis periods. The observed features include
243 sudden spikes in concentrations of trace gases, aerosol particles, and BC. These observations agree with the
244 previous studies showing a connection between holiday-related firework celebrations and degraded air quality
245 (Jiang et al., 2015; Yang et al., 2014; Shi et al., 2014; Feng et al., 2012; Zhang et al., 2010). In the sections
246 below, we will delve into these results, which can broaden scientific understanding of the impacts of firework

247 celebrations on local and regional air quality, especially in the context of a wide metropolitan area over the
248 course of several years.

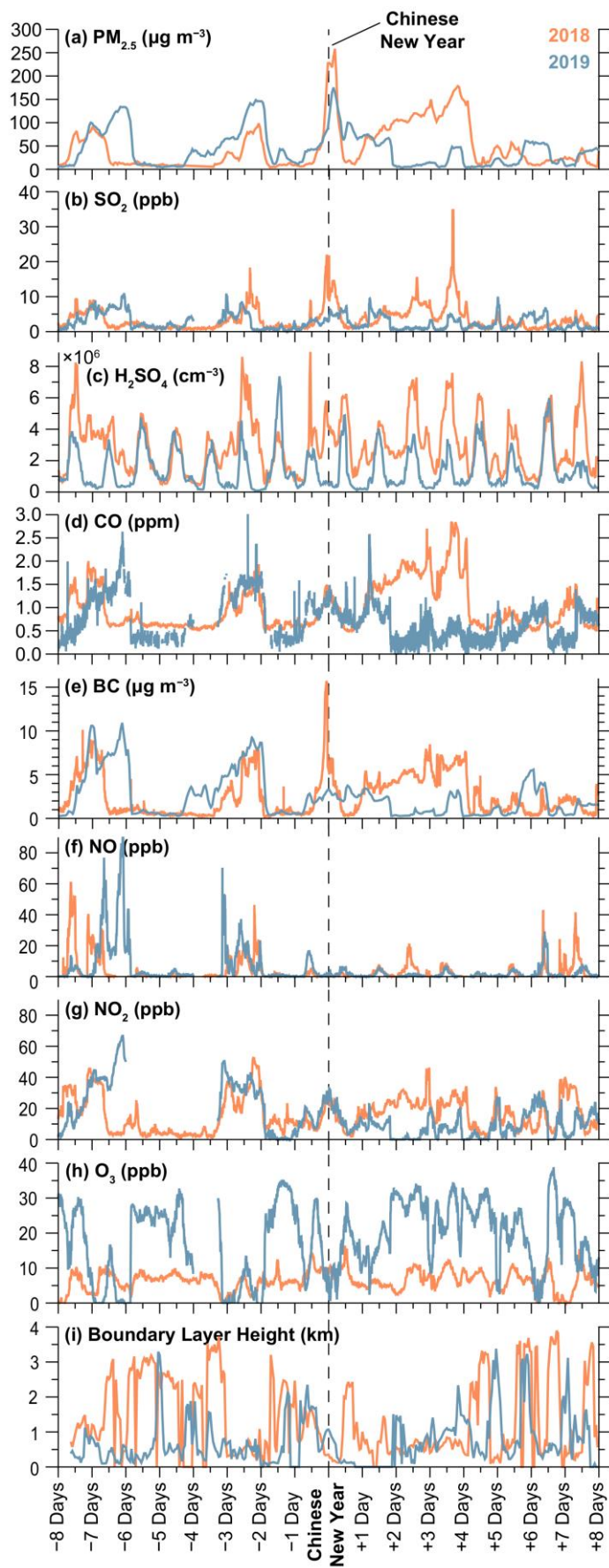
249

250 **3.1 Characteristics of air quality during the Chinese New Years 2018 and 2019**

251

252 The CNY was on February 16, 2018 and February 5, 2019. Figure 2 shows a timeseries of air pollutant
253 concentrations from eight days before to eight days after the 2018 and 2019 CNY at BUCT-AHL (except for
254 $PM_{2.5}$, which is from the nearby MEP sites). We observed sharp peaks in Particulate Matter mass ($PM_{2.5}$), SO_2 ,
255 sulfuric acid, CO, BC, NO, and NO_2 and ozone during firework events. In 2018 the peak in $PM_{2.5}$ was over 250
256 $\mu g/m^3$, compared to less than 50 $\mu g/m^3$ half a day before, and in 2019 the peak of $PM_{2.5}$ was over 150 $\mu g/m^3$
257 compared to less than 100 $\mu g/m^3$ earlier in the day. Similar spikes in BC, gas phase sulfuric acid, and trace gas
258 concentrations of several times the values earlier in the day were observed in 2018 as well.

259



261 **Figure 2: Concentrations of main pollutants measured and Boundary Layer Height in Beijing**
262 **during the 2018 CNY (orange) and 2019 CNY (blue)**

263
264 In contrast, in 2019, PM_{2.5} was observed to have less noticeable enhancement in concentration. While there
265 was a noticeable spike in SO₂ overnight of the CNY in 2018 (a spike over 20 ppb compared to less than 5 ppb
266 earlier in the day), shown in Figure 2, a much less noticeable enhancement of SO₂ was observed overnight of
267 the 2019 CNY (a peak around 5 ppb compared to around 3 ppb earlier in the day).

268
269 The measurements showed elevated nighttime concentration of H₂SO₄ on CNY in 2018 exceeding 3·10⁶ cm⁻³
270 during the whole night, which was an order of magnitude higher than typical nighttime H₂SO₄ concentrations
271 of 5·10⁵ cm⁻³ (Dada et al., 2020). In 2019, there was no evident indication of anomalies in nighttime H₂SO₄
272 concentration during CNY. An unknown spike in H₂SO₄ was noticed at noon the day before CNY in 2018, and
273 its association with celebratory activities is unclear. Like with PM_{2.5} and SO₂, Figure 2 shows a distinctive
274 spike in BC around midnight of the 2018 CNY. Although SO₂ and BC also originate from coal combustion and
275 other emission sources (Wang et al., 2018), because of the shortness of the peak, and the fact that it occurs at
276 exactly midnight, these simultaneous peaks of BC and SO₂ during the nighttime of CNY most likely originate
277 from firework burning.

278
279 However, there appeared to be little to no effect of CNY on BC in 2019. The measurements showed an elevated
280 concentration of NO₂ overnight of the CNY in both years (45 ppb in 2018 and 20 ppb in 2019), yet no obvious
281 spike in NO concentration. A high NO₂/NO_x ratio can be caused by accumulation of pollutants emitted the
282 previous afternoon (Chou et al., 2009), but in case of CNY night it is straight forward to conclude it is due to
283 firework burning, which has been shown to emit NO₂ but no NO (Jiang et al., 2015).

284
285 Figure 2 also shows that during the CNY celebrations in 2018 concentrations of the primary pollutants, SO₂,
286 CO, BC, NO and NO₂, were elevated, implying enhanced direct emissions during the CNY period. Secondary
287 pollutants are formed through chemical reactions (Seinfeld and Pandis, 2016) including, for instance, sulfuric
288 acid and ozone. The concentrations of these secondary pollutants were as expected: sulfuric acid concentration
289 increased due to enhanced formation rate with increased SO₂ concentration, and ozone concentration decreased
290 with increased chemical sink by NO_x and CO (and probably other carbon compounds). However, in 2019, only
291 the concentrations of CO and NO₂ were observed to increase during CNY celebrations, leading to a decrease
292 in ozone concentration.

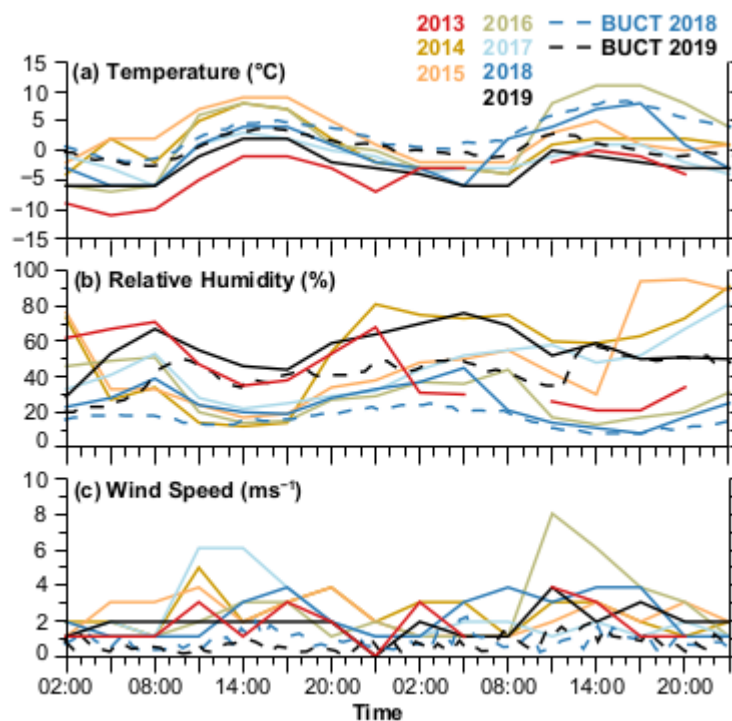
293
294 Interestingly, in addition to the short-term enhancement of pollutant concentrations, Figure 2 shows degraded
295 air quality between 16-20 February 2018, following the Chinese New Year, which closely resembles the
296 characteristics of a haze event as described in Zhao et al. (2013), Zhao et al. (2011) and Guo et al. (2020). Using
297 the data from BUCT-AHL, this period was quantifiably classified as a haze event using the algorithm in Zhou
298 et al. (2020). These haze events have elevated concentrations of pollution continuously for multiple days, and
299 concentrations gradually increase throughout the episodes. The haze eventually ends with sudden decline, often
300 caused by an arrival of a cold front or change in synoptic weather conditions. Several previous studies,
301 including Jiang et al. (2015) and Li et al. (2013), suggest that fireworks likely contribute to haze formation. It
302 is plausible that the increased level of pollutants observed overnight during the 2018 CNY likely contributed
303 to this subsequent haze period. However, the meteorological conditions and air mass origins are also important
304 for haze formation, which are discussed in Section 3.2.

305
306 **3.2 Effects of Meteorology and Boundary Layer Height**

308 Because the meteorological conditions during CNY vary between different years, it is important to address the
 309 impact of local and synoptic scale meteorological parameters on air pollution when comparing different years
 310 to each other. Specifically, wind speed and direction, relative humidity (RH), boundary layer height, and
 311 precipitation can affect pollutant concentrations during and after the fireworks.

312
 313 However, none of the measured local meteorological variables showed drastic differences between CNY nights
 314 of 2018 and 2019. The wind speed during the night of the 2018 CNY peaked at ~ 2 m/s, and during the night of
 315 the 2019 CNY, it remained to values less than ~ 1 m/s (Figure 3 and Figure S1 in Supplementary). Temperature
 316 was between 0 and 5 $^{\circ}\text{C}$ on both years. Some difference was observed in relative humidity, as CNY 2018 took
 317 place in very dry conditions (RH $\sim 20\%$), whereas during CNY 2019 RH was roughly 40%. Precipitation was
 318 not measured at BUCT-AHL in either year, and weather data measured at ZBNY show there was no
 319 precipitation in the region during either of the years (data obtained from Weather Underground), which was
 320 supported by observed RH values below 50%. The nocturnal boundary layer heights were less than 500 meters
 321 in both years (Figure 2), which is unfavorable for vertical mixing of the pollutants. Due to the slightly lower
 322 wind speeds in 2019 than 2018, we would expect more efficient dispersion of pollutants, and thus lower
 323 concentrations in 2018. Higher RH is also often related to higher concentrations of aerosol pollutants (Sun et
 324 al., 2013). However, what we observed was that there were higher concentrations in 2018 than 2019. This
 325 indicates that the reason for lower pollutant concentrations in 2019 is not due to differences in the local
 326 meteorological conditions.

327



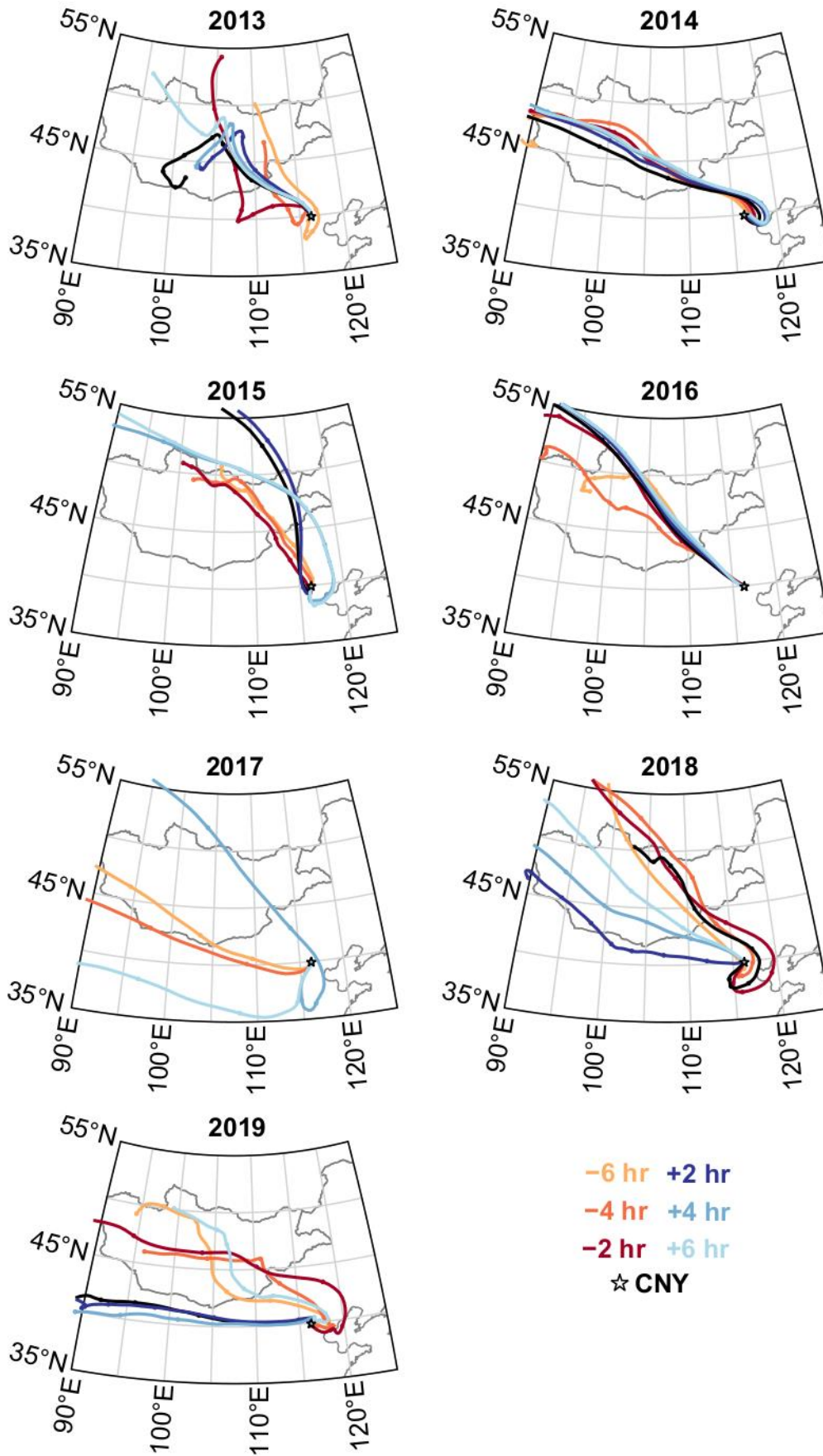
328
 329 **Figure 3:** Meteorological conditions during CNY night \pm one day measured in Beijing from 2013-
 330 2019. Solid lines are measurements from Beijing Nanyuan Airport (ZBNY). These measurements are
 331 every three hours. Dashed lines are measurements at BUCT-AHL during 2018-2019, with time
 332 resolution of one hour.

333
 334 The lower concentrations observed during the emission spike in 2019 can be either due to lower emission rates
 335 in the area with which the measured air mass is in contact, or due to a shorter exposure to roughly similar
 336 emissions during both years. Figure 4 shows 96 hour back-trajectories by Hysplit, during the night of CNY in

337 2018 and 2019, showing the sources of the airmasses. This provides further insights into the history of the
338 airmasses in Beijing, including how clean we can expect the airmasses to be before CNY, and whether the
339 airmasses are stagnant around Beijing or whether clean air is being transported into the city.

340
341 These trajectories show the following: In 2018, the airmasses from six hours prior to CNY through CNY are
342 from the southwest, and from two through six hours after CNY, the airmass is from the west. In 2019, airmasses
343 from six hours prior to CNY through two hours prior to CNY the airmasses are from the east, and following
344 the CNY the airmasses are primarily from the west.

345
346 Based on Wang et al. (2019), airmasses from the east are expected to be cleaner than from the southwest due
347 to more diffusion and less emissions from industry. However, we observed the opposite: From six through two
348 hours prior to midnight (i.e. the background value before the spike in pollution), the background pollutant
349 concentrations are higher in 2019 than in 2018. This gives further indication that the emission sources are likely
350 localized and short-term as opposed to long-range transport.



352 **Figure 4:** Hysplit 96 hour back-trajectories for air masses arriving at BUCT-AHL between 18:00
353 and 06:00 local time, the night of CNY in 2013 through 2019. The markers are every 12 hours.

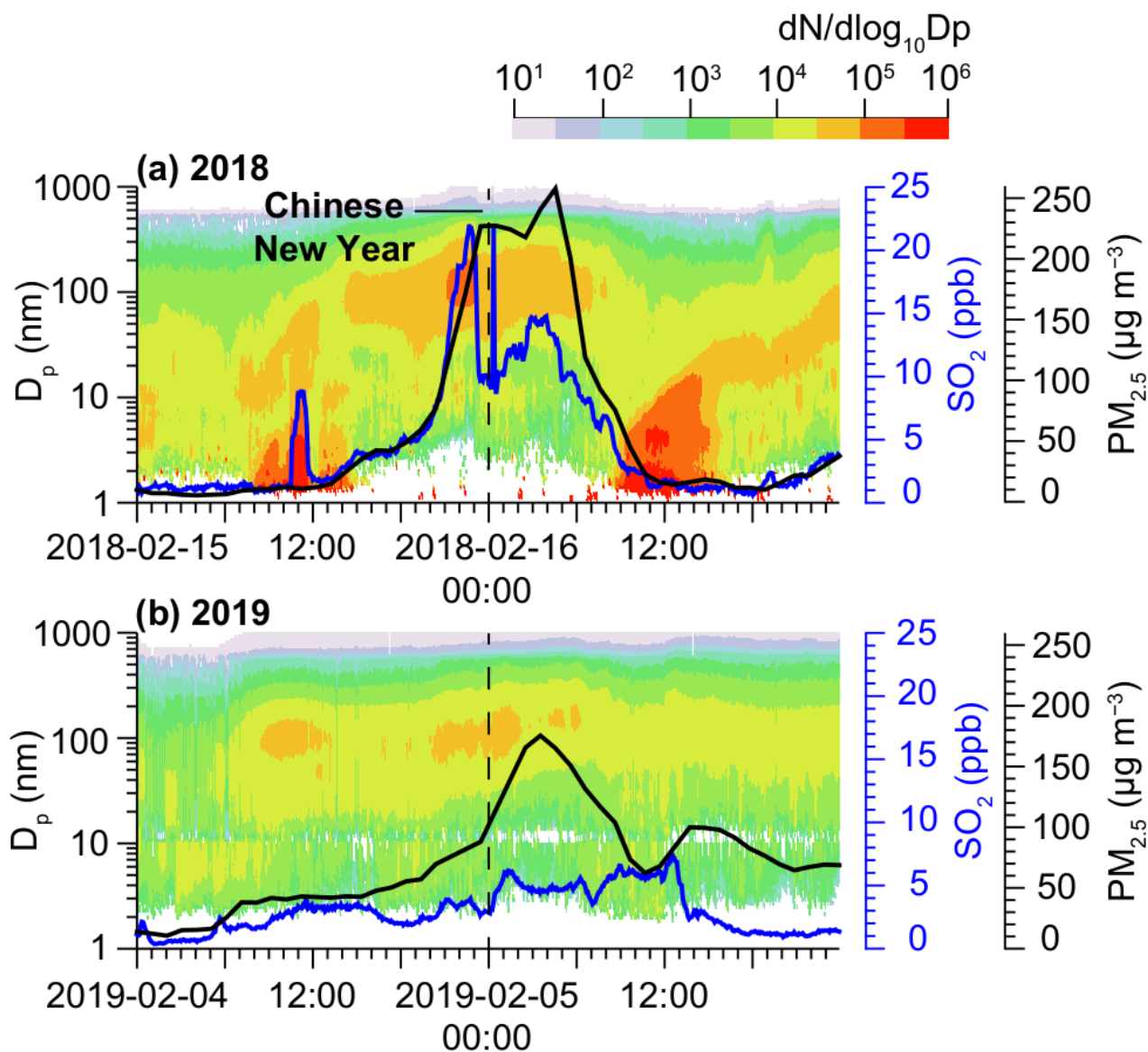
354

355 **3.3 Aerosol particle number concentrations and aerosol number size distribution**

356

357 Further exploring the effects of the fireworks on air pollution, Figure 5 shows PSD at BUCT-AHL from the
358 day before to the day after CNY. Shortly before midnight on CNY in 2018, an elevated concentration of aerosol
359 particles with diameters of roughly 100 nm was observed, simultaneous to the spike in SO₂ concentration. After
360 the spike, SO₂ concentration remained elevated until the next morning. PM_{2.5} concentration increases
361 simultaneously with the SO₂ concentration but did not show the same spike as SO₂. PM_{2.5} concentration
362 remained high (>200 µg/m³) until the next morning, when it decreased to low values (<30 µg/m³) together with
363 decreasing SO₂ concentration. The nocturnal pollution episode showed a very similar pattern in both SO₂ and
364 PM_{2.5}, despite the spike in SO₂ occurring together with increased number concentration of roughly 100 nm
365 particles and BC (Figure 2e). This is consistent with air pollution from firework burning. It might have
366 originated from a source nearby, but it can also be transported as a single strong plume from further away, e.g.,
367 from outside the 5th Ring Road which was the edge of the prohibited area for firework activity. The overnight
368 elevated concentration of PM_{2.5} and SO₂, excluding the SO₂ spike, may be related to accumulated mixture of
369 firework and other festivity related emissions, e.g., from traffic or cooking. The accumulation of PM_{2.5} seems
370 to be related to secondary aerosol formation, since the particle size distribution shows growth of particles in
371 the dominant particle mode during the CNY night (concentration dN/d(log(d_p)) over 3.3·10⁴ between diameters
372 40 and 200 nm at around 8 pm and between diameters 60 and close to 300 nm at around 4 am).

373

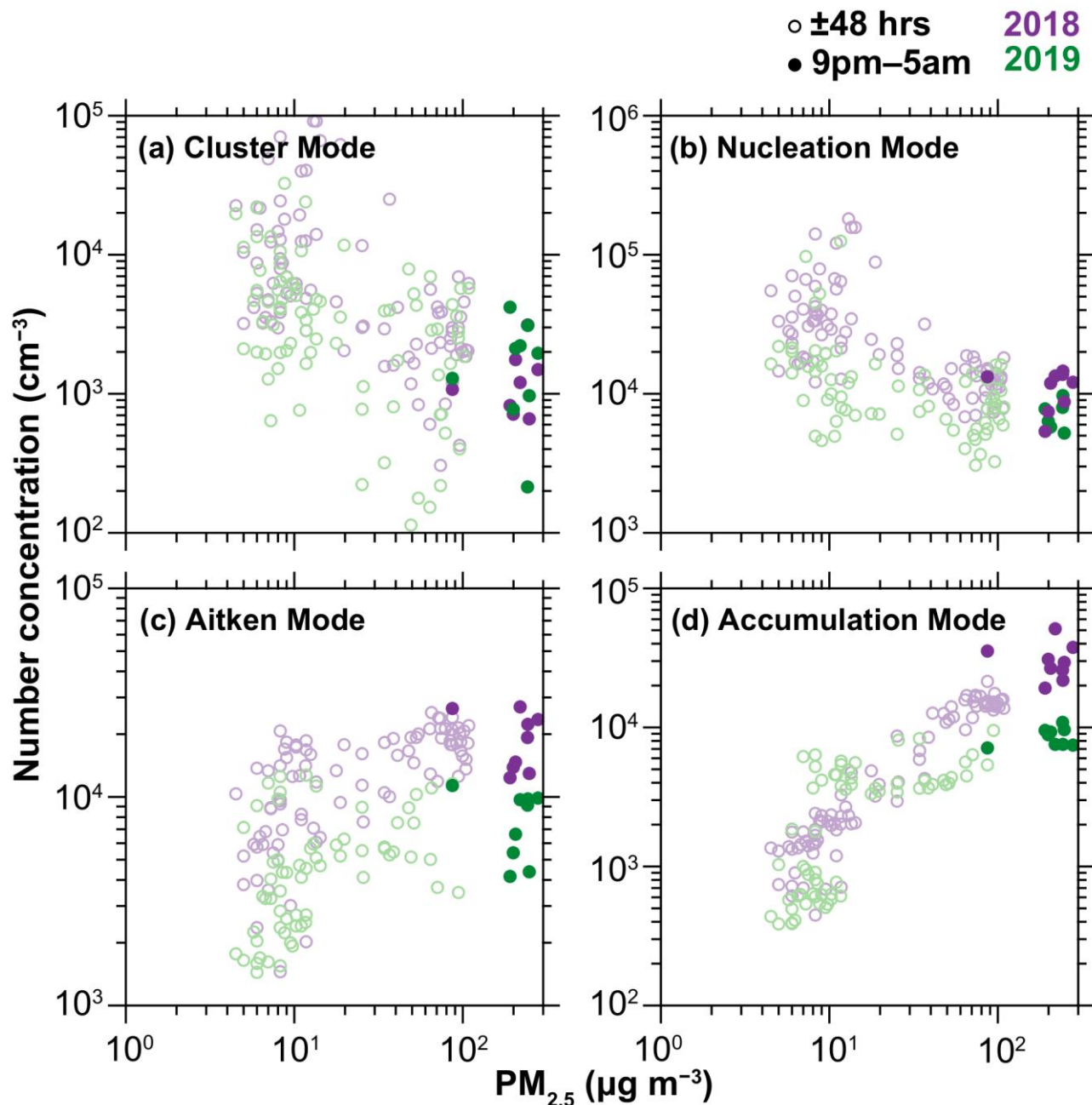


374
 375 **Figure 5:** Aerosol particle number size distribution (PSD) from one day before the CNY through one day
 376 following the CNY in 2018 and 2019, overlain with aerosol mass concentration $PM_{2.5}$ (black lines) and SO_2
 377 (blue lines).

378
 379 In 2019, secondary aerosol mass formation was also observed, as the particle mode grew in diameter steadily
 380 between 6 pm and 6 am and the $PM_{2.5}$ concentration increased simultaneously until 4 am. The peak $PM_{2.5}$
 381 concentration was, however, much lower in 2019 than in 2018 (roughly 100 $\mu g m^{-3}$ and close to 250 $\mu g m^{-3}$,
 382 respectively). SO_2 increased steadily throughout the night and exhibited only a mild peak, from 3 to 6 ppb,
 383 shortly after midnight. This peak was again accompanied with simultaneous increase in concentration of
 384 particles with diameters around 100 nm and in BC concentration (Figure 2), which suggests contribution from
 385 fireworks. However, since the SO_2 concentration showed only a mild peak and did not follow the $PM_{2.5}$
 386 concentration, the contribution of nearby firework activity to the overall pollution was estimated to be
 387 negligible.

388
 389 Figure 6 shows the particle number concentrations in four size modes, specifically sub-3 nm cluster mode, 3-
 390 25 nm nucleation mode, 25-100 nm Aitken mode, and 100-1000 nm accumulation mode, as a function $PM_{2.5}$

391 concentration measured at BUCT-AHL in 2018 and 2019. This figure starts 48 hours before CNY and runs
392 through 48 hours after the CNY. The filled circles mark the nighttime measurements on the CNY (9pm-5am).
393 The night-time mass concentrations are noticeably greater. The mass-to-number concentration comparison for
394 CNY follows the same general curve during nighttime as the full time period. The pattern, particularly the
395 nighttime observations, is consistent with recent investigation by Zhou et al. (2020), which showed that in
396 general concentrations of pollutants are higher during nighttime, attributed to a lower boundary layer and
397 consequent high concentrations within the boundary layer. As noted in Section 3.1, the $PM_{2.5}$ concentrations
398 during the CNY period in 2018 were nearly an order of magnitude higher than before and after this time. The
399 elevated $PM_{2.5}$ concentration is directly connected to the elevated number concentration of accumulation mode
400 particles (Fig. 6 bottom right panel) and the CNY data points do not diverge from the overall coupling. This
401 indicates that the typical sizes of particles contributing to $PM_{2.5}$ remains similar during CNY than before and
402 after it. Since the accumulation mode particle concentrations form the main part of the total particle surface
403 acting as a condensation sink for vapors forming new particles in the atmosphere and a coagulation sink for
404 small cluster and nucleation mode particles, it is natural that the concentrations of cluster and nucleation mode
405 decrease with increasing $PM_{2.5}$ (Fig. 6, upper panels).
406

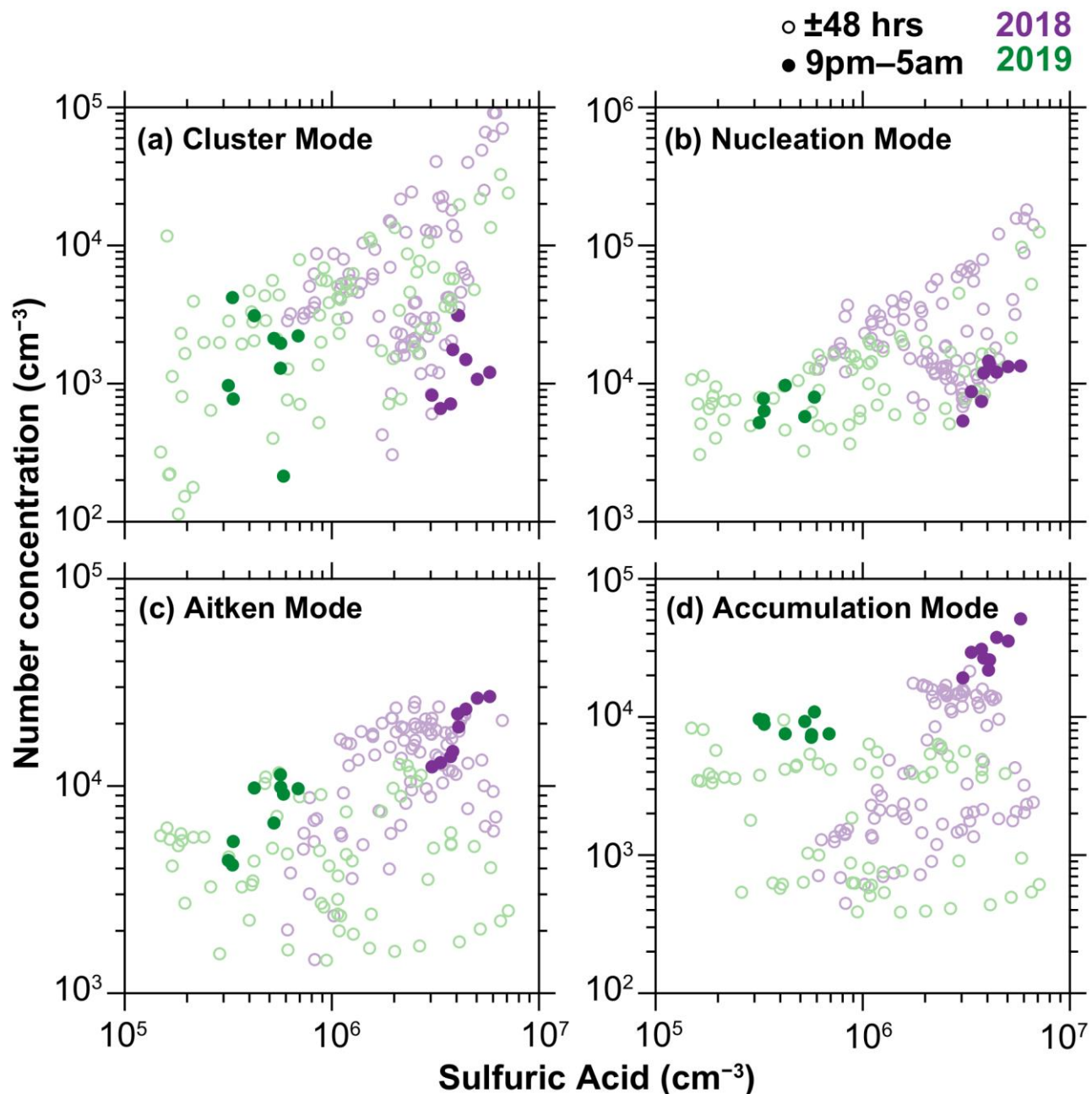


407
 408 **Figure 6:** Aerosol particle number concentrations in cluster, nucleation, Aitken and accumulation modes as a
 409 function of PM_{2.5} mass concentration in 2018 (purple) and 2019 (green), separated from 9pm through 5am the
 410 night of the CNY (filled circles) and those of CNY ± 48 hours (open circles). The data is from BUCT-AHL.
 411

412 In short, the CNY activities seem not to cause any major deviance for the typical aerosol dynamics other than
 413 the enhancement of the source of accumulation mode particles
 414

415 Figure 7 depicts the cluster, nucleation, Aitken and accumulation mode particle number concentrations as a
 416 function of gas phase sulfuric acid concentration in 2018 and in 2019 inside and outside of the CNY period.
 417 Looking at the clusters, the results show a general strong dependency on the sulfuric acid as it is one of the
 418 main pre-cursors driving the process of gas-to-particle conversion (e.g, Sipilä et al. 2010, Kulmala et al. 2013,
 419 Yao et al. 2018). However, the high nocturnal sulfuric acid concentration during CNY celebrations in 2018

420 does not lead to high cluster or nucleation mode concentration. In fact, the particle number concentrations in
 421 these modes deviates from the otherwise clear response to sulfuric acid concentrations. The reason for this is
 422 visible in the panel for accumulation mode concentration vs sulfuric acid concentration: during the CNY 2018
 423 the high concentrations of accumulation mode particles correlates with sulfuric acid concentration thus
 424 plausibly neglecting the enhanced particle cluster and particle formation rates by enhanced coagulation sink as
 425 explained earlier.
 426



427
 428 **Figure 7:** Aerosol particle number concentrations in cluster, nucleation, Aitken and accumulation modes as a
 429 function of gas phase sulfuric acid concentration in 2018 (purple) and 2019 (green), separated from 9pm
 430 through 5am the night of the CNY (filled circles) and those of CNY ± 48 hours (open circles). The data is from
 431 BUCT-AHL.
 432

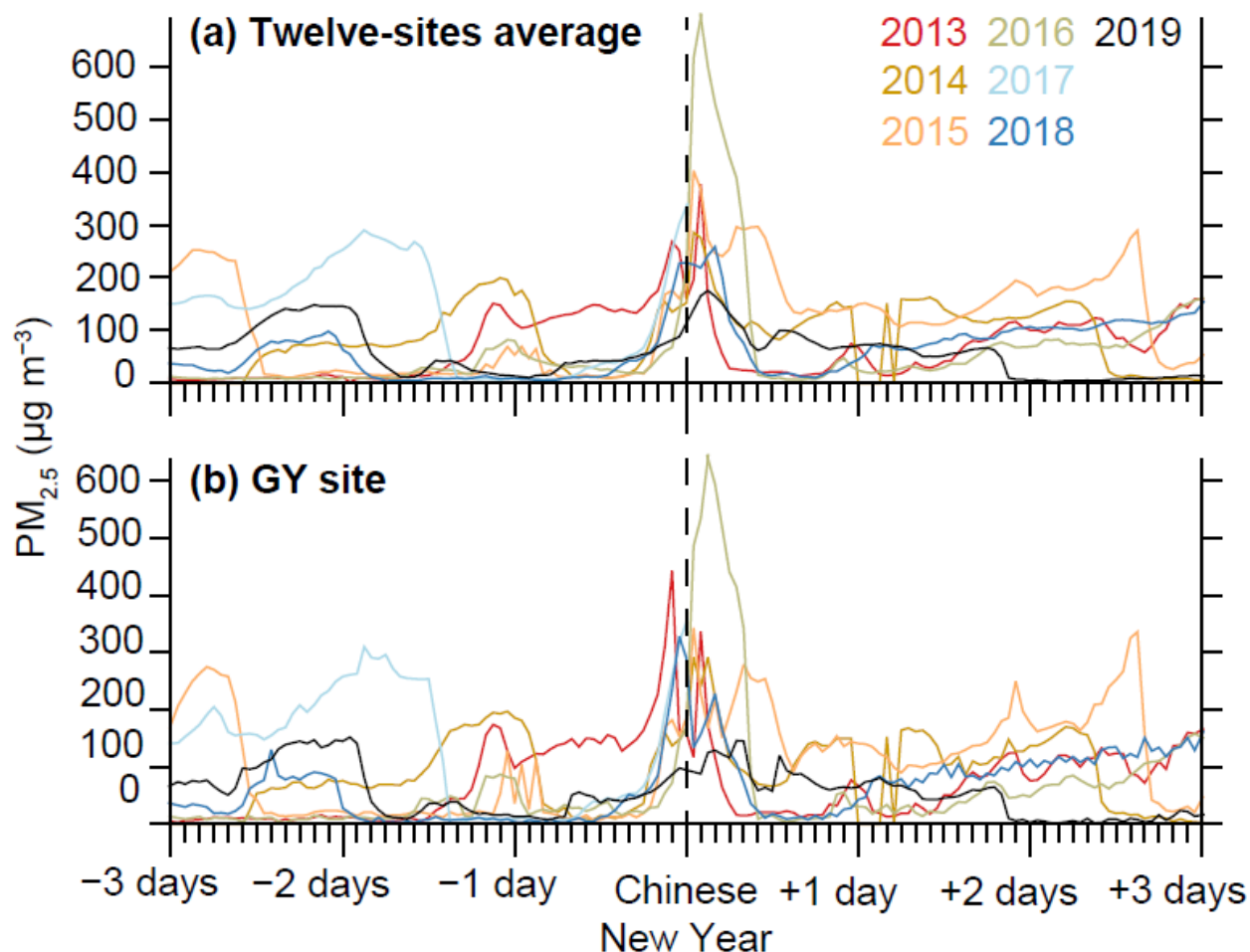
433 **3.4 Multi-Year Variation of Chinese New Year Effects in Beijing**

434
435 Fireworks were formally prohibited within the 5th Ring Road of Beijing beginning in 2018, whereas outside
436 the 5th Ring Road, there were no prohibitions (Liu et al., 2019). Still, there was some evidence of firework
437 burning observed BUCT-AHL, which is within the prohibition area.

438
439 A longer-term multi-year study can be useful in demonstrating whether or not the policy is effective in reducing
440 firework-related pollution, and if there is an overall decreasing trend of pollution effects from fireworks over
441 multiple years. To investigate this question, it is useful to compare the 2018 and 2019 CNY with previous years
442 in Beijing. Datasets have been analyzed from 12 MEP stations in the Beijing area from 2013 through 2019.

443
444 Figure 8 shows that each year, there was a spike in pollution around midnight during the CNY. The highest
445 levels were observed in 2016, with the peak in PM_{2.5} around midnight of the CNY reaching almost 700 µg/cm³
446 while values earlier in the day were less than 100 µg/cm³. The lowest levels of PM_{2.5} were in 2019 with the
447 overnight peak less than 200 µg/cm³ compared to daytime values around 50 µg/cm³. Observations from 2013,
448 2014, 2015, and 2017 also showed similarly high or higher levels of PM_{2.5} as in 2018 (unfortunately the 2017
449 dataset is incomplete and does not extend beyond 00:00 of New Years day due to a network outage). The
450 measurements for all seven years are in agreement with other studies that have linked elevated air pollution
451 levels to CNY celebrations (Yang et al., 2014; Shi et al., 2014; Feng et al., 2012; Zhang et al., 2010), and this
452 study further shows that the peak in 2019 is lower than in 2018, which is lower than in 2016 and 2017.

453



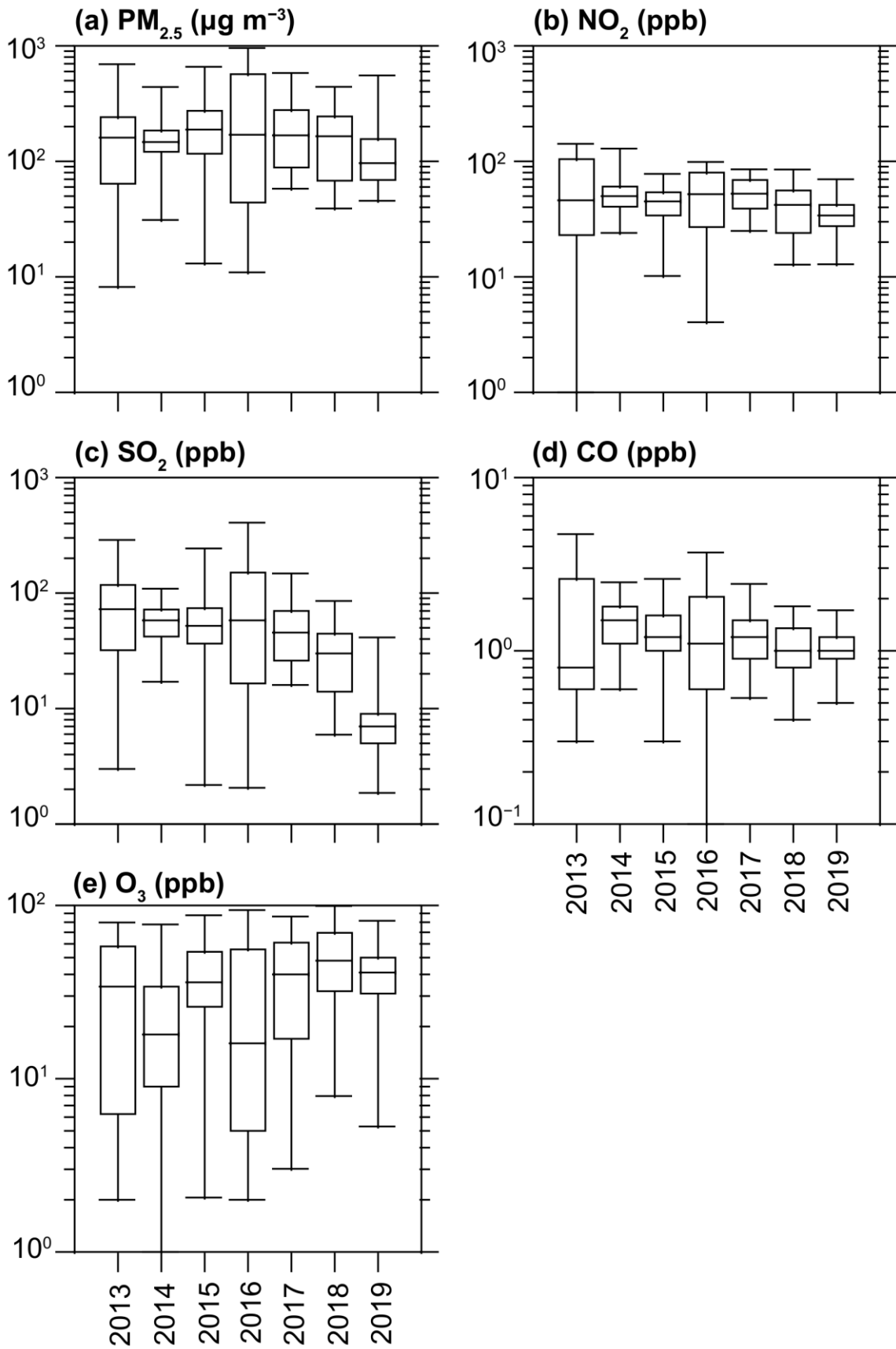
454

455 **Figure 8:** PM_{2.5} averaged from 12 MEP sites in Beijing (top) and from only the Guanyuan (GY) site, which is
456 the closest MEP measurement site to BUCT-AHL (bottom), from three days before through three days after
457 the 2013-2019 CNY. The highest peak of pollution during the CNY overnight was in 2016, and the lowest was
458 in 2019.

459
460 Data from the CNYs have also been compiled into box plots in Figure 9, depicting the distributions of pollutant
461 concentrations from 6:00 pm on CNY Eve to 6:00 am on the CNY day each year at all 12 MEP stations. The
462 highest PM concentrations during this time were in 2016, and the 75th and 99th percentile concentrations have
463 decreased after that. On the other hand, the median concentration remained high during 2017 and 2018 but
464 decreased in 2019 by roughly a factor of two. Concentrations of NO₂ and SO₂ show a more steady decrease
465 than PM_{2.5}, since the median concentration of both pollutants decreased steadily from 2016 (regarding NO₂ for
466 2017), but for CO there is no clear pattern. It should be noted that in 2017, the data is missing after midnight
467 due to an unknown network outage. The more noticeable decrease in NO₂ and SO₂ is an expected outcome for
468 a ban on firework burning, since both are produced by fireworks and have shorter lifetimes than CO and PM_{2.5}
469 (Seinfeld and Pandis, 2016; Lee et al., 2011). Thus, they are less affected by long range transport and
470 accumulation. The decrease in pollutant concentrations since 2016 agrees with the results obtained by Liu et
471 al. (2019). Since ozone is a secondary product and it reacts with several primary pollutants, its concentration
472 pattern being roughly opposite to those of primary pollutants is as expected.

473

New Years Eve (6pm–6am)



475 **Figure 9:** Boxplots of PM_{2.5} and trace gases between 18:00 and 06:00 on the night of the Chinese New Year in
476 the years 2013-2019. The boxplots show 1st, 25th, 50th, 75th, and 99th percentiles of the data across the 12 sites
477 during this 12-hour period (13 time points, inclusively).
478

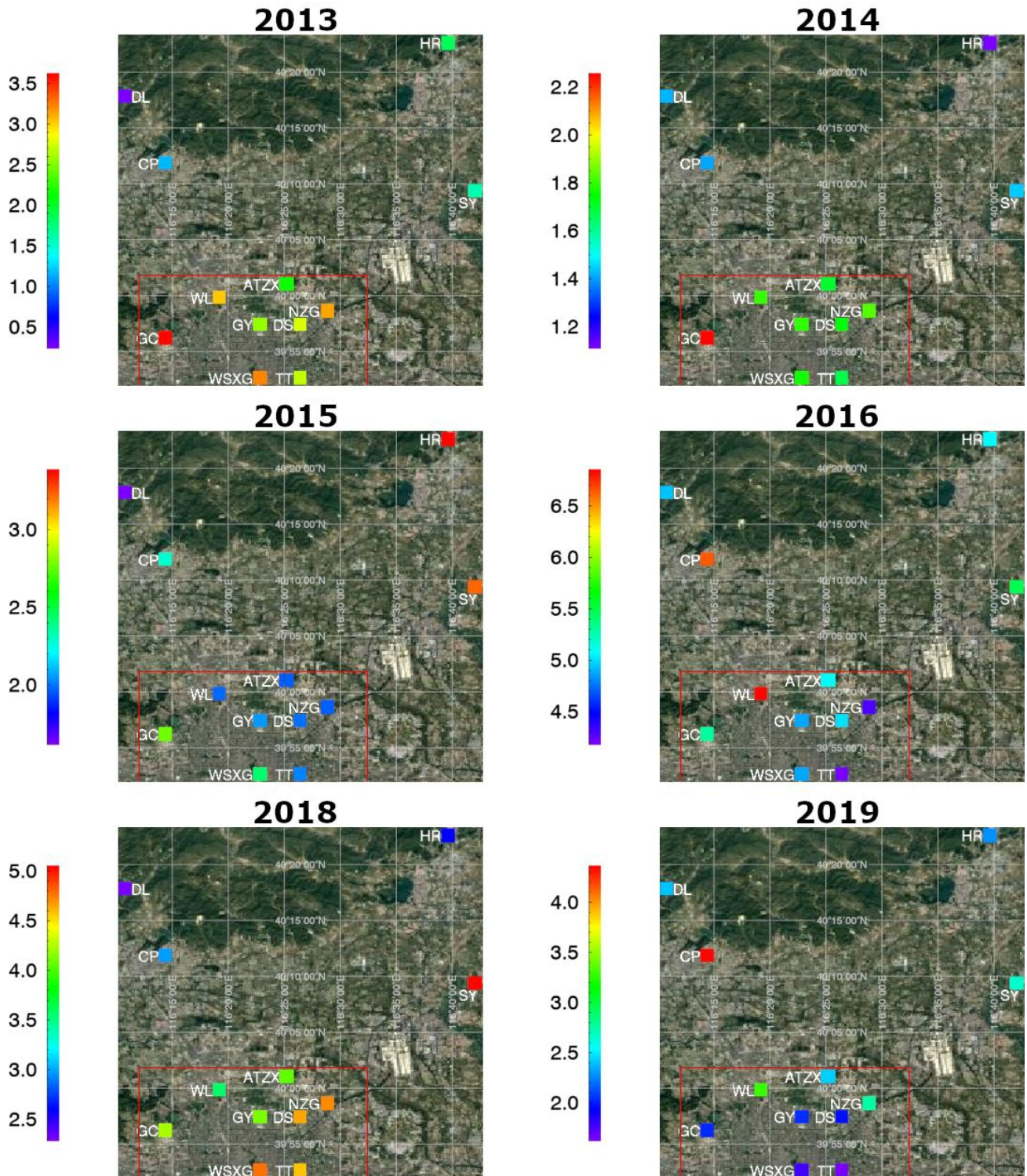
479 Based on Hysplit back-trajectories (Figure 4), we see that in 2013-2015 the airmasses spent longer in the BTH
480 area prior to arrival. This differs from the airmass sources in 2016-2017, where the airmasses come directly
481 from the northwest. These areas to the northwest of Beijing, including Inner Mongolia and Mongolia usually
482 contain less pollutants due to low anthropogenic emissions, and thus we can expect air masses from this region
483 to be cleaner (Xu et al., 2008). Based on the airmass history, if emissions were the same, then there should be
484 higher concentrations in 2013-2015; however, we see the highest concentrations of pollutants in 2016, followed
485 by a decline after that. In 2018 and 2019, the airmasses spent around two days in the BTH area leading up to
486 arrival at the station. Based on airmass source alone, we would have expected higher pollutant concentrations
487 in 2018 and 2019, but this is not the case. Thus, we can conclude that emissions must have been highest in
488 2016, with lower emissions in 2018 and 2019. This agrees with Liu et al. (2019).
489

490 **3.5 Spatial variability based on MEP measurement network data**

491

492 Next, we performed a spatial comparison of the MEP measurements across the Beijing region. This includes
493 comparing the observations inside the 5th Ring Road, where fireworks were prohibited, to outside the ring.
494 Figure 10 maps the 12 MEP stations in the Beijing region for 2013-2019, showing the ratio between mean
495 PM_{2.5} concentration from 9 pm through 5 am during the night of CNY and the mean concentration within ± 48
496 hours of the CNY at each site. Figures S2-S13 in Supplementary Information show observations of PM_{2.5} from
497 the 12 individual MEP sites and the corresponding differences, year-by-year from 2013-2019. Based on Figure
498 10, we can see significant variation from year to year as to which station measures the highest pollution. It is
499 important to note that the population density is greater closer to city center, and thus the population density
500 could impact the results. However, it is plausible to assume that the relative population density difference
501 between the city center and the surrounding areas do not change dramatically during the few years' time period.
502

PM_{2.5} Relative Differences: Overnight Average / Average of \pm 48 hours



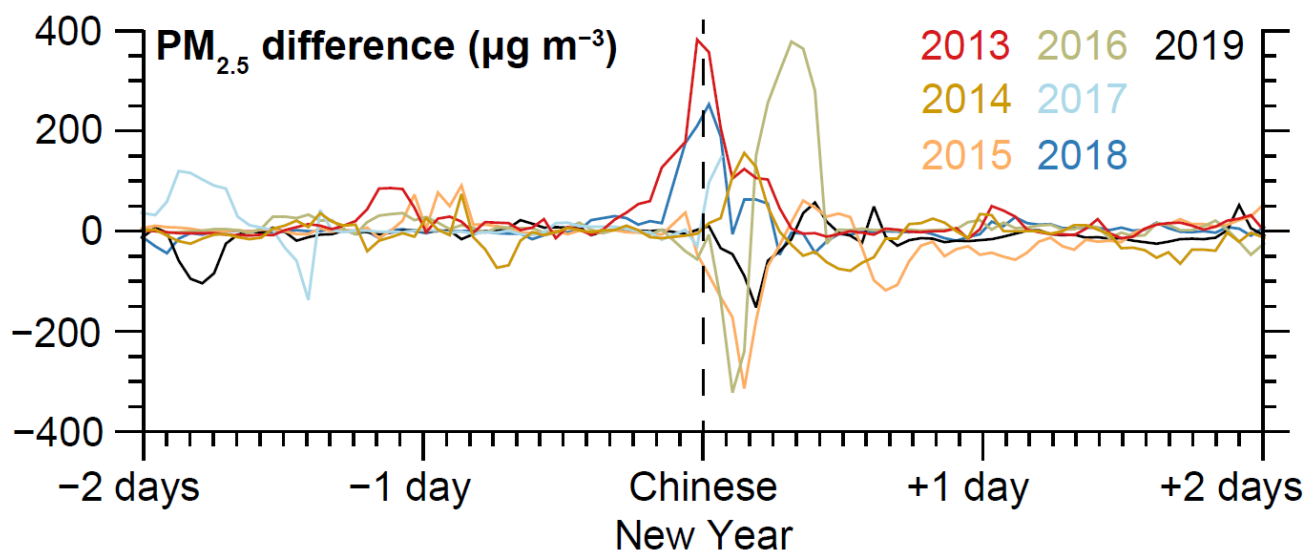
503
 504 **Figure 10:** The 12 MEP sites mapped in the Beijing metropolitan area, showing the ratio of overnight PM_{2.5}
 505 observations during the CNY (21:00-05:00) to all data during the period of 48 hours before through 48 hours
 506 after the CNY. The red line marks the approximate location of the 5th Ring Road. Note that the colorbars in
 507 each map are relative to only that year, and the colorbar range is not the same in different years. 2017 is omitted

508 from this figure because data after 00:00 was not available. A list of the sites' full names in English and Chinese,
509 along with their latitude and longitude coordinates can be found in Table S1 in Supplementary material.
510 Imagery: © Google Earth.

511
512 Figure 10 illustrates that in 2013 and 2014, the enhancement in $PM_{2.5}$ concentrations during CNY is greater
513 inside the 5th ring than outside. In 2015, the enhancement is much greater at the two northeastern sites (HR and
514 SY). In 2016, the differences vary, with no clear difference inside or outside the 5th ring. In 2018, the
515 enhancement of $PM_{2.5}$ is higher inside the 5th ring than outside, except for the SY site to the far northeast, which
516 had significantly high enhancement compared to the other sites. In 2019 the enhancement is overall less inside
517 compared to outside. The enhancement factors outside the 5th Ring road (excluding the single highest value)
518 and at the Northern inside stations nearest to the Ring road are quite similar in 2019, roughly in range 2.5 to 3,
519 but the peak times of pollution are few hours earlier at the outside stations than the Northern inside stations
520 (Fig. S12). The measurement sites closer to central Beijing, on the other hand, show clearly lower enhancement
521 factors, of values of two or below. Based on these spatial and temporal differences, and on the northerly winds
522 observed at the time, it is possible that the higher enhancement factors inside but close to the 5th Ring road are
523 related to emissions from outside the Ring road.

524
525 Figure 11 shows differences between the $PM_{2.5}$ mean of the sites inside the 5th Ring Road and the mean of the
526 sites outside the 5th Ring (that is the mean of the 8 inside sites minus the mean of the outside 4 stations) 48
527 hours before through 48 hours after the CNY for 2013-2019. In 2013, 2014 and 2018, the enhancement of $PM_{2.5}$
528 during the CNY overnight is greater inside than outside the 5th Ring Road. However, in 2015 and 2019, as well
529 as immediately after the CNY midnight in 2016, $PM_{2.5}$ was lower inside than outside. While we were lacking
530 the detailed data on local meteorology during 2013-2016, we were still able to analyze the meteorological
531 condition in terms of air mass trajectories. Figure 4 shows that, similar to 2019 as discussed previously, in 2015
532 and CNY midnight of 2016, airmasses arriving to Beijing were from the cleaner West-North sector and arrived
533 with much higher velocity in comparison to years 2013, 2014 and 2018, during which the air masses made a
534 turn in South or East before arrival to Beijing. Even though the CNYs during which the increase of $PM_{2.5}$
535 enhancement inside the 5th Ring Road is less pronounced than outside seem to be related to faster arrival of
536 cleaner airmasses, we have no clear view for the reason of this difference and, due to the qualitative nature of
537 this comparison, it is well possible that this connection is pure coincidence. The similarity of years 2015 and
538 2019 in terms of the spatial variation of CNY midnight pollution peak suggests that meteorology may be at
539 least part of the reason for the lesser enhancement of pollution levels inside the 5th Ring Road than outside.
540 Nevertheless, the notably lower concentrations of $PM_{2.5}$ and gaseous air pollutants in 2019 than in 2015
541 indicates that, even with similarities in spatial distribution of changes in concentrations, the most likely reason
542 for lower concentrations during CNY night are the lower emissions.

543



544 **Figure 11:** Differences between mean PM_{2.5} concentrations inside and outside the 5th Ring Road of Beijing
 545 from 2013 through 2019. Positive values indicate higher concentration inside 5th Ring Road.
 546

547
 548 **4 CONCLUSIONS**

549
 550 In this study, we looked at comprehensive measurements over CNY 2018 and 2019 at a measurement station
 551 in Beijing, along with long-term datasets across the Beijing metropolitan area.
 552

553 Our study confirms that CNY consistently impacts air quality in Beijing. Based on our observations at the
 554 BUCT-AHL station in Beijing, in 2018, we detected higher than typical night-time concentrations of particulate
 555 mass (PM_{2.5}), particle number, trace gas and sulfuric acid concentrations during the CNY. This was expected,
 556 and these results are consistent with previous studies that have linked the CNY (and other similar holiday
 557 celebrations involving firework burning around the world) to degraded air quality both locally and regionally.
 558

559 Our results suggest that the regulations from CNY 2018 to limit firework use have improved the air quality
 560 within the restriction zone inside the 5th Ring road in Beijing, and from 2016 to 2019 there has been a decrease
 561 in the effects of holiday-related pollution, which offers an optimistic outlook to the air quality impacts caused
 562 by CNY and the consequential public health concerns stemming from air pollution.
 563

564 During the CNY night in 2018, we observed appearance of particles with diameters of roughly 100 nm that
 565 seemed to be linked to enhanced sulfur dioxide, sulfuric acid and black carbon concentrations, most likely as a
 566 result from firework burning. Based on the MEP data, the peaks in concentrations of different pollutants were
 567 lower than in the previous years. In 2019, a peak in pollution was observed overnight, but it was significantly
 568 lower than in 2018, while meteorological conditions were comparable in both years. The significant year-to-
 569 year variability depended presumably on the meteorological conditions. A common phenomenon for both 2018
 570 and 2019 CNY nights was the accumulation of secondary aerosol throughout the night, seen as a diameter
 571 growth of the dominant particle mode in particle number size distributions. Measurements at BUCT-AHL
 572 showed that in 2018 a moderate haze episode began one day following the CNY, potentially related to the
 573 firework burning.
 574

575 Comparing the level of increase in pollutant concentrations during CNY night inside Beijing's 5th ring road
 576 (firework prohibition area) to outside revealed that in 2019 the increase inside this area was smaller than
 577 outside. During most – but not all – of the previous CNYs, the increase in concentration was higher inside than

578 outside. This was also the case in 2018. However, as also in previous years the ratio of inside and outside
579 concentrations during CNY has varied, it is unclear if this is related to efficacy of the emission prohibition or,
580 e.g., to larger scale air-mass movements, or simply due to the fact that fireworks are sporadic and localized
581 emission sources. Nonetheless, in terms of absolute concentrations, our results show a decrease of CNY
582 pollution within the prohibition area since 2016 and especially in 2019. This is in agreement with the previous
583 Liu et al. (2019) study, which compared the 2016 and 2018 CNY (before and after the prohibition took effect).
584

585 To conclude, this long-term analysis, which combines BUCT data with multiple years of Chinese government
586 data at 12 locations in the Beijing area, demonstrates the importance of analyzing multiple data sources to
587 determine overall trends, rather than making conclusions based on a single dataset. This also demonstrates the
588 usefulness of long-term measurements. Using these datasets together, we see excellent potential that can be
589 utilized to investigate the changes in a) atmospheric chemistry – such as ozone dynamics and sulfuric acid
590 formation; b) atmospheric gas-to-particle conversion; c) boundary layer dynamics and d) air quality. Using
591 CNY as a case study offers excellent insight into how rapid changes in emissions will affect air quality, health,
592 and quality of life, especially in megacities such as Beijing. To confirm and quantify the influence of banning
593 the firework burning in Beijing and the impact of varying meteorological conditions, similar data from coming
594 CNYs is needed. Therefore, we suggest ongoing measurements at both BUCT-AHL and MEP sites into
595 multiple future years.

596

597 **Acknowledgements**

598

599 The work is supported by Academy of Finland via Center of Excellence in Atmospheric Sciences (project no.
600 272041) and European Research Council via ATM-GTP 266 (742206). This research has also received funding
601 from Academy of Finland (project no. 316114 & 315203, 307537), Business Finland via Megasense-project,
602 European Commission via SMart URBan Solutions for air quality, disasters and city growth, (689443), ERA-
603 NET-Cofund as well as the Doctoral Programme in Atmospheric Sciences at the University of Helsinki. Partial
604 support from the National Key R&D Program of China (2016YFC0200500), and the National Natural Science
605 Foundation of China (91544231 & 41725020) is acknowledged. The authors also wish to acknowledge the
606 Finnish Centre for Scientific Computing (CSC) – IT Center for Science, Finland, for computational resources.

607

608 **Author Contributions**

609

610 All BUCT affiliated authors, plus KD, BC, YW, TC, and PR contributed to measurement collection at BUCT.
611 LW provided the quality-controlled MEP data. BF, LD, KD, TP, FB, PP and MK conceptualized and conducted
612 the data analysis. TK, MoK, RP, and RB participated in the data analysis. TK and MoK provided the
613 meteorology data. KD, TP, FB, PP and MK supervised the study. BF visualized the data with assistance from
614 SG. BF wrote the original draft and prepared the manuscript. PP, TP and all other authors reviewed and edited
615 the manuscript.

616

617 **Competing Interests**

618

619 The authors declare that there are no conflicts of interest in this study.

620

621 **Data Availability**

622

623 Data from the BUCT station is available at request. Real time data from the MEP stations is available at
624 <http://106.37.208.233:20035/>. Archived, quality-controlled MEP data may also be available upon request.

625

626 **REFERENCES**

- 627
- 628 Bach, W., Daniels, A., Dickinson, L., Hertlein, F., Morrows, J., Margolis, S. and Dinh, V.: Fireworks pollution
629 and health, *International Journal of Environmental Studies*, 7(3), 183-192, doi:10.1080/00207237508709692,
630 2007.
- 631 Barman, S., Singh, R., Negi, M. and Bhargava, S.: Ambient air quality of Lucknow City (India) during use of
632 fireworks on Diwali Festival, *Environ. Monit. and Assess.*, 137(1-3), 495-504, doi:10.1007/s10661-007-9784-
633 1, 2007.
- 634 Chen, B., Kan, H., Chen, R., Jiang, S. and Hong, C.: Air Pollution and Health Studies in China—Policy
635 Implications, *Journal of the Air & Waste Management Association*, 61(11), 1292-1299,
636 doi:10.1080/10473289.2011.604288, 2011.
- 637 Chen, Z., Zhang, J., Zhang, T., Liu, W. and Liu, J.: Haze observations by simultaneous lidar and WPS in
638 Beijing before and during APEC, 2014, *Sci. China. Chem.*, 58(9), 1385-1392, doi:10.1007/s11426-015-5467-
639 x, 2015.
- 640 Chou, C., Tsai, C., Shiu, C., Liu, S. and Zhu, T.: Measurement of NO_y during Campaign of Air Quality
641 Research in Beijing 2006 (CAREBeijing-2006): Implications for the ozone production efficiency of NO_x, *J.*
642 *Geophys. Res.*, 114, doi:10.1029/2008jd010446, 2009.
- 643 Dada, L., Ylivinkka, I., Baalbaki, R., Li, C., Guo, Y., Yan, C., Yao, L., Sarnela, N., Jokinen, T., Daellenbach,
644 K., Yin, R., Deng, C., Chu, B., Nieminen, T., Wang, Y., Lin, Z., Thakur, R., Kontkanen, J., Stolzenburg, D.,
645 Sipilä, M., Hussein, T., Paasonen, P., Bianchi, F., Salma, I., Weidinger, T., Pikridas, M., Sciare, J., Jiang, J.,
646 Liu, Y., Petäjä, T., Kerminen, V. and Kulmala, M.: Sources and sinks driving sulfuric acid concentrations in
647 contrasting environments: implications on proxy calculations, *Atmos. Chem. Phys.*, 20(20), 11747-11766,
648 doi:10.5194/acp-20-11747-2020, 2020.
- 649 Feng, J., Sun, P., Hu, X., Zhao, W., Wu, M. and Fu, J.: The chemical composition and sources of PM_{2.5}
650 during the 2009 Chinese New Year's holiday in Shanghai, *Atmos. Res.*, 118, 435-444,
651 doi:10.1016/j.atmosres.2012.08.012, 2012.
- 652 Hari, P. & Kulmala, M.: Station for measuring Ecosystem-Atmosphere relations (SMEAR II). *Boreal*
653 *Environ. Res.*, 10., 315-322, 2005.
- 654 He, H., Li, C., Loughner, C., Li, Z., Krotkov, N., Yang, K., Wang, L., Zheng, Y., Bao, X., Zhao, G. and
655 Dickerson, R.: SO₂ over central China: Measurements, numerical simulations and the tropospheric sulfur
656 budget, *J. Geophys. Res.: Atmospheres*, 117(D16), n/a-n/a, doi:10.1029/2011jd016473, 2012.
- 657 Heintzenberg, J., Wehner, B. and Birmili, W.: 'How to find bananas in the atmospheric aerosol': new
658 approach for analyzing atmospheric nucleation and growth events, *Tellus B*, 59(2),
659 doi:10.3402/tellusb.v59i2.16988, 2007.
- 660 Jiang, Q., Sun, Y., Wang, Z. and Yin, Y.: Aerosol composition and sources during the Chinese Spring
661 Festival: fireworks, secondary aerosol, and holiday effects, *Atmos. Chem. Phys.*, 15(11), 6023-6034,
662 doi:10.5194/acp-15-6023-2015, 2015.
- 663 Kong, S., Li, L., Li, X., Yin, Y., Chen, K., Liu, D., Yuan, L., Zhang, Y., Shan, Y. and Ji, Y., 2015. The
664 impacts of firework burning at the Chinese Spring Festival on air quality: insights of tracers, source evolution
665 and aging processes. *Atmos. Chem. Phys.*, 15(4), pp.2167-2184.

- 666 Kong, S., Li, L., Li, X., Yin, Y., Chen, K., Liu, D., Yuan, L., Zhang, Y., Shan, Y. and Ji, Y.: The impacts of
667 firework burning at the Chinese Spring Festival on air quality: insights of tracers, source evolution and aging
668 processes, *Atmos. Chem. Phys.*, 15(4), 2167-2184, doi:10.5194/acp-15-2167-2015, 2015.
- 669 Kulmala, M., Kontkanen, J., Junninen, H., Lehtipalo, K., Manninen, H., Nieminen, T., Petäjä, T., Sipilä, M.,
670 Schobesberger, S., Rantala, P., Franchin, A., Jokinen, T., Järvinen, E., Äijälä, M., Kangasluoma, J., Hakala,
671 J., Aalto, P., Paasonen, P., Mikkilä, J., Vanhanen, J., Aalto, J., Hakola, H., Makkonen, U., Ruuskanen, T.,
672 Mauldin, R., Duplissy, J., Vehkamäki, H., Bäck, J., Kortelainen, A., Riipinen, I., Kurtén, T., Johnston, M.,
673 Smith, J., Ehn, M., Mentel, T., Lehtinen, K., Laaksonen, A., Kerminen, V. and Worsnop, D.: Direct
674 Observations of Atmospheric Aerosol Nucleation, *Science*, 339(6122), 943-946,
675 doi:10.1126/science.1227385, 2013.
- 676 Kulmala, M.: Atmospheric chemistry: China's choking cocktail, *Nature*, 526(7574), 497-499,
677 doi:10.1038/526497a, 2015.
- 678 Kulmala, M., 2018. Build a global Earth observatory. *Nature*, 553(7686), pp.21-23.
- 679 Kulmala, M., Kerminen, V., Petäjä, T., Ding, A. and Wang, L.: Atmospheric gas-to-particle conversion: why
680 NPF events are observed in megacities?, *Faraday Discuss.*, 200, 271-288, doi:10.1039/c6fd00257a, 2017.
- 681 Kürten, A., Rondo, L., Ehrhart, S. and Curtius, J.: Calibration of a Chemical Ionization Mass Spectrometer
682 for the Measurement of Gaseous Sulfuric Acid, *J. Phys. Chem. A.*, 116(24), 6375-6386,
683 doi:10.1021/jp212123n, 2012.
- 684 Lee, C., Martin, R., van Donkelaar, A., Lee, H., Dickerson, R., Hains, J., Krotkov, N., Richter, A., Vinnikov,
685 K. and Schwab, J.: SO₂ emissions and lifetimes: Estimates from inverse modeling using in situ and global,
686 space-based (SCIAMACHY and OMI) observations, *J. Geophys. Res.*, 116(D6), doi:10.1029/2010jd014758,
687 2011.
- 688 Li, W., Shi, Z., Yan, C., Yang, L., Dong, C. and Wang, W.: Individual metal-bearing particles in a regional
689 haze caused by firecracker and firework emissions, *Sci. Total. Environ.*, 443, 464-469,
690 doi:10.1016/j.scitotenv.2012.10.109, 2013.
- 691 Liu, D., Rutherford, D., Kinsey, M. and Prather, K.: Real-Time Monitoring of Pyrotechnically Derived
692 Aerosol Particles in the Troposphere, *Anal. Chem.*, 69(10), 1808-1814, doi:10.1021/ac9612988, 1997.
- 693 Liu, J., Chen, Y., Chao, S., Cao, H. and Zhang, A.: Levels and health risks of PM_{2.5}-bound toxic metals from
694 firework/firecracker burning during festival periods in response to management strategies, *Ecotoxicology and*
695 *Environ. Safe.*, 171, 406-413, doi:10.1016/j.ecoenv.2018.12.104, 2019.
- 696 Liu, J., Jiang, J., Zhang, Q., Deng, J. and Hao, J.: A spectrometer for measuring particle size distributions in
697 the range of 3 nm to 10 μm, *Front. Env. Sci. Eng.*, 10(1), 63-72, doi:10.1007/s11783-014-0754-x, 2014.
- 698 Liu, Y., Yan, C., Feng, Z., Zheng, F., Fan, X., Zhang, Y., Li, C., Zhou, Y., Lin, Z., Guo, Y., Zhang, Y., Ma,
699 L., Zhou, W., Liu, Z., Dada, L., Dällenbach, K., Kontkanen, J., Cai, R., Chan, T., Chu, B., Du, W., Yao, L.,
700 Wang, Y., Cai, J., Kangasluoma, J., Kokkonen, T., Kujansuu, J., Rusanen, A., Deng, C., Fu, Y., Yin, R., Li,
701 X., Lu, Y., Liu, Y., Lian, C., Yang, D., Wang, W., Ge, M., Wang, Y., Worsnop, D., Junninen, H., He, H.,
702 Kerminen, V., Zheng, J., Wang, L., Jiang, J., Petäjä, T., Bianchi, F. and Kulmala, M.: Continuous and
703 comprehensive atmospheric observations in Beijing: a station to understand the complex urban atmospheric
704 environment, *Big Earth Data*, 4(3), 295-321, doi:10.1080/20964471.2020.1798707, 2020.

705 Mönkkönen, P., Koponen, I., Lehtinen, K., Uma, R., Srinivasan, D., Hämeri, K. and Kulmala, M.: Death of
706 nucleation and Aitken mode particles: observations at extreme atmospheric conditions and their theoretical
707 explanation, *J. Aerosol Sci.*, 35(6), 781-787, doi:10.1016/j.jaerosci.2003.12.004, 2004.

708 Peltonen, M.: University of Helsinki builds an air quality measuring station in Beijing | University of
709 Helsinki, [online] Available from: [https://www.helsinki.fi/en/news/climate-change-and-](https://www.helsinki.fi/en/news/climate-change-and-biodiversity/university-helsinki-builds-air-quality-measuring-station-beijing)
710 [biodiversity/university-helsinki-builds-air-quality-measuring-station-beijing](https://www.helsinki.fi/en/news/climate-change-and-biodiversity/university-helsinki-builds-air-quality-measuring-station-beijing) (Accessed 22 January 2022),
711 2017.

712 Ravindra, K., Mor, S. and Kaushik, C.: Short-term variation in air quality associated with firework events: A
713 case study, *Journal of Environ. Monitor.*, 5(2), 260-264, doi:10.1039/b211943a, 2003.

714 Seinfeld, J. and Pandis, S.: *Atmospheric Chemistry and Physics: From Air Pollution to Climate Change*, 3rd
715 Edition, 3rd ed., Wiley, ISBN: 978-1-118-94740-1, 2016.

716 Shen, X., Sun, J., Zhang, Y., Wehner, B., Nowak, A., Tuch, T., Zhang, X., Wang, T., Zhou, H., Zhang, X.,
717 Dong, F., Birmili, W. and Wiedensohler, A.: First long-term study of particle number size distributions and
718 new particle formation events of regional aerosol in the North China Plain, *Atmos. Chem. Phys.* 11(4), 1565-
719 1580, doi:10.5194/acp-11-1565-2011, 2011.

720

721 Shi, G., Liu, G., Tian, Y., Zhou, X., Peng, X. and Feng, Y.: Chemical characteristic and toxicity assessment
722 of particle associated PAHs for the short-term anthropogenic activity event: During the Chinese New Year's
723 Festival in 2013, *Sci. Total Environ.*, 482-483, 8-14, doi:10.1016/j.scitotenv.2014.02.107, 2014.

724 Singh, D., Gadi, R., Mandal, T., Dixit, C., Singh, K., Saud, T., Singh, N. and Gupta, P.: Study of temporal
725 variation in ambient air quality during Diwali festival in India, *Environ. Monit. Asses.*, 169(1-4), 1-13,
726 doi:10.1007/s10661-009-1145-9, 2009.

727 Sipilä, M., Berndt, T., Petäjä, T., Brus, D., Vanhanen, J., Stratmann, F., Patokoski, J., Mauldin, R.,
728 Hyvärinen, A., Lihavainen, H. and Kulmala, M.: The Role of Sulfuric Acid in Atmospheric Nucleation,
729 *Science*, 327(5970), 1243-1246, doi:10.1126/science.1180315, 2010.

730 Song, C., Wu, L., Xie, Y., He, J., Chen, X., Wang, T., Lin, Y., Jin, T., Wang, A., Liu, Y., Dai, Q., Liu, B.,
731 Wang, Y. and Mao, H.: Air pollution in China: Status and spatiotemporal variations, *Environ. Pollut.*, 227,
732 334-347, doi:10.1016/j.envpol.2017.04.075, 2017.

733 Stein, A., Draxler, R., Rolph, G., Stunder, B., Cohen, M. and Ngan, F.: NOAA's HYSPLIT Atmospheric
734 Transport and Dispersion Modeling System, *B. Am. Soc.*, 96(12), 2059-2077, doi:10.1175/bams-d-14-
735 00110.1, 2015.

736 Sun, Y., Wang, Z., Fu, P., Jiang, Q., Yang, T., Li, J. and Ge, X.: The impact of relative humidity on aerosol
737 composition and evolution processes during wintertime in Beijing, China, *Atmos. Environ.*, 77, 927-934,
738 doi:10.1016/j.atmosenv.2013.06.019, 2013.

739 Tao, M., Chen, L., Li, R., Wang, L., Wang, J., Wang, Z., Tang, G. and Tao, J.: Spatial oscillation of the
740 particle pollution in eastern China during winter: Implications for regional air quality and climate, *Atmos.*
741 *Environ.*, 144, 100-110, doi:10.1016/j.atmosenv.2016.08.049, 2016.

742 van der A, R., Mijling, B., Ding, J., Koukouli, M., Liu, F., Li, Q., Mao, H. and Theys, N.: Cleaning up the air:
743 effectiveness of air quality policy for SO₂ and
744 NO_x emissions in China, *Atmos. Chem. Phys.*, 17(3), 1775-1789,
745 doi:10.5194/acp-17-1775-2017, 2017.

746 Vanhanen, J., Mikkilä, J., Lehtipalo, K., Sipilä, M., Manninen, H., Siivola, E., Petäjä, T. and Kulmala, M.:
747 Particle Size Magnifier for Nano-CN Detection, *Aerosol Sci. Tech.*, 45(4), 533-542,
748 doi:10.1080/02786826.2010.547889, 2011.

749 Virkkula, A., Chi, X., Ding, A., Shen, Y., Nie, W., Qi, X., Zheng, L., Huang, X., Xie, Y., Wang, J., Petäjä, T.
750 and Kulmala, M.: On the interpretation of the loading correction of the aethalometer, *Atmos. Meas. Tech.*,
751 8(10), 4415-4427, doi:10.5194/amt-8-4415-2015, 2015.

752 Wang, F., Chen, D., Cheng, S., Li, J., Li, M. and Ren, Z.: Identification of regional atmospheric PM10
753 transport pathways using HYSPLIT, MM5-CMAQ and synoptic pressure pattern analysis, *Environ. Modell.*
754 *Softw.*, 25(8), 927-934, doi:10.1016/j.envsoft.2010.02.004, 2010.

755 Wang, Y., Zhuang, G., Xu, C. and An, Z.: The air pollution caused by the burning of fireworks during the
756 lantern festival in Beijing, *Atmos. Environ.*, 41(2), 417-431, doi:10.1016/j.atmosenv.2006.07.043, 2007.

757 Wang, Y., Dörner, S., Donner, S., Böhnke, S., De Smedt, I., Dickerson, R., Dong, Z., He, H., Li, Z., Li, Z.,
758 Li, D., Liu, D., Ren, X., Theys, N., Wang, Y., Wang, Y., Wang, Z., Xu, H., Xu, J. and Wagner, T.: Vertical
759 profiles of NO₂, SO₂, HONO, HCHO, CHOCHO and
760 aerosols derived from MAX-DOAS measurements at a rural site in the central western North China Plain and
761 their relation to emission sources and effects of regional transport, *Atmos. Chem. Phys.*, 19(8), 5417-5449,
762 doi:10.5194/acp-19-5417-2019, 2019.

763 Wang, Y., Li, Z., Zhang, Y., Du, W., Zhang, F., Tan, H., Xu, H., Fan, T., Jin, X., Fan, X., Dong, Z., Wang, Q.
764 and Sun, Y.: Characterization of aerosol hygroscopicity, mixing state, and CCN activity at a suburban site in
765 the central North China Plain, *Atmos. Chem. Phys.*, 18(16), 11739-11752, doi:10.5194/acp-18-11739-2018,
766 2018.

767 Beijing, People's Republic Of China Weather History | Weather Underground, Wunderground.com [online]:
768 <https://www.wunderground.com/history/weekly/cn/beijing/ZBNY/date/2019-2-4> (Accessed 22 January
769 2022), 2022.

770 Wu, H., Tang, X., Wang, Z., Wu, L., Lu, M., Wei, L. and Zhu, J.: Probabilistic Automatic Outlier Detection
771 for Surface Air Quality Measurements from the China National Environmental Monitoring Network, *Adv.*
772 *Atmos. Sci.*, 35(12), 1522-1532, doi:10.1007/s00376-018-8067-9, 2018.

773 Xu, X., Barsha, N. and Li, J.: Analyzing Regional Influence of Particulate Matter on the City of Beijing,
774 China, *Aerosol Air Qual. Res.*, 8(1), 78-93, doi:10.4209/aaqr.2007.09.0038, 2008.

775 Xue, W., Wang, J., Niu, H., Yang, J., Han, B., Lei, Y., Chen, H. and Jiang, C.: Assessment of air quality
776 improvement effect under the National Total Emission Control Program during the Twelfth National Five-
777 Year Plan in China, *Atmos. Environ.*, 68, 74-81, doi:10.1016/j.atmosenv.2012.11.053, 2013.

778 Yang, L., Gao, X., Wang, X., Nie, W., Wang, J., Gao, R., Xu, P., Shou, Y., Zhang, Q. and Wang, W.: Impacts
779 of firecracker burning on aerosol chemical characteristics and human health risk levels during the Chinese
780 New Year Celebration in Jinan, China, *Sci. Total Environ.*, 476-477, 57-64,
781 doi:10.1016/j.scitotenv.2013.12.110, 2014.

782 Yao, L., Garmash, O., Bianchi, F., Zheng, J., Yan, C., Kontkanen, J., Junninen, H., Mazon, S., Ehn, M.,
783 Paasonen, P., Sipilä, M., Wang, M., Wang, X., Xiao, S., Chen, H., Lu, Y., Zhang, B., Wang, D., Fu, Q.,
784 Geng, F., Li, L., Wang, H., Qiao, L., Yang, X., Chen, J., Kerminen, V., Petäjä, T., Worsnop, D., Kulmala, M.
785 and Wang, L.: Atmospheric new particle formation from sulfuric acid and amines in a Chinese megacity,
786 *Science*, 361(6399), 278-281, doi:10.1126/science.aao4839, 2018.

- 787 Yerramsetti, V., Sharma, A., Gauravarapu Navlur, N., Rapolu, V., Dhulipala, N. and Sinha, P.: The impact
788 assessment of Diwali fireworks emissions on the air quality of a tropical urban site, Hyderabad, India, during
789 three consecutive years, *Environ. Monit. Asses.*, 185(9), 7309-7325, doi:10.1007/s10661-013-3102-x, 2013.
- 790 Zhang, M., Wang, X., Chen, J., Cheng, T., Wang, T., Yang, X., Gong, Y., Geng, F. and Chen, C.: Physical
791 characterization of aerosol particles during the Chinese New Year's firework events, *Atmos. Environ.* 44(39),
792 5191-5198, doi:10.1016/j.atmosenv.2010.08.048, 2010.
- 793 Zhao, X., Zhao, P., Xu, J., Meng, W., Pu, W., Dong, F., He, D. and Shi, Q.: Analysis of a winter regional
794 haze event and its formation mechanism in the North China Plain, *Atmos. Chem. Phys.*, 13(11), 5685-5696,
795 doi:10.5194/acp-13-5685-2013, 2013.
- 796 Zhao, X., Zhang, X., Pu, W., Meng, W. and Xu, X.: Scattering properties of the atmospheric aerosol in
797 Beijing, China, *Atmos. Res.*, 101(3), 799-808, doi:10.1016/j.atmosres.2011.05.010, 2011.
- 798 Zhou, Y., Dada, L., Liu, Y., Fu, Y., Kangasluoma, J., Chan, T., Yan, C., Chu, B., Daellenbach, K., Bianchi,
799 F., Kokkonen, T., Liu, Y., Kujansuu, J., Kerminen, V., Petäjä, T., Wang, L., Jiang, J. and Kulmala, M.:
800 Variation of size-segregated particle number concentrations in wintertime Beijing, *Atmos. Chem. Phys.*,
801 20(2), 1201-1216, doi:10.5194/acp-20-1201-2020, 2020.
- 802 Zhu Y. Y., Gao Y. X., Chai W. X., Wang, S., Li, L., Wang, W., Wang, G., Liu, B., Wang, X. Y., Li, J. J.:
803 Analysis of regional heavy PM_{2.5} pollution events in Beijing-Tianjin-Hebei and the surrounding area in
804 China during 2015–2018, *Global NEST J.*, doi:10.30955/gnj.003589, 2021.